ELECTRONIC STRUCTURE OF (CATECHOLATO)(1,10-PHENANTHROLINE)COPPER(II): INTRAMOLECULAR INTERLIGAND ELECTRONIC INTERACTIONS

Yasunori Yamada[a]; Toshihiko Hoshi[a]; Yutaka Fukuda[b]

[a] Department of Chemistry, College of Science and Engineering, Aoyama Gakuin University, Tokyo, Setagaya-ku, Japan [b] Department of Chemistry, Faculty of Science, Ochanomizu University, Tokyo, Bunkyo-Ku, Japan

PLEASE SCROLL DOWN FOR ARTICLE

ELECTRONIC STRUCTURE OF (CATECHOLATO) (1,10-PHENANTHROLINE)COPPER(II): INTRAMOLECULAR INTERLIGAND ELECTRONIC INTERACTIONS

YASUNORI YAMADA, TOSHIHIKO HOSHI,*

*Department of Chemistry, College of Science and Engineering, Aoyama Gakuin University,
Chitosedai 6–16–1, Setagaya-ku, Tokyo 157, Japan*

and YUTAKA FUKUDA

*Department of Chemistry, Faculty of Science, Ochanomizu University, Otsuka 3–3–6, Bunkyo-Ku,
Tokyo 112, Japan*

The electronic absorption spectrum of (catecholato)(1,10-phenanthroline)copper(II) ([Cu(cat)(phen)]) measured in 1:1 methanol and water was compared with those of (catecholato)(ethylenediamine)copper(II) ([Cu(cat)(en)]) and (oxalato)(1,10-phenanthroline)copper(II) ([Cu(ox)(phen)]). From the above results together with MO calculations and polarization spectra using stretched PVA films, it is found that the 330, 295.0, 275.0, 267, 233, and 223 nm bands of [Cu(cat)(phen)] are due to transitions localized on the phen moiety, and the 292 and 210.0 nm bands on the cat moiety. The 209 nm band of [Cu(cat)(phen)] can be interpreted as arising from a mixture of two kinds of transitions localized on phen and cat. This implies that the two π-electronic systems, being usually considered to exist independently on the two moieties, can interact greatly, as newly reported here.

INTRODUCTION

Mixed ligand complexes with labile metal ions have attracted great interest for many years from the synthetic and physicochemical points of view. Among these complexes, ternary copper(II) complexes have been studied extensively by Sigel and co-workers, especially from bioinorganic view points.[1–11] It is well known that ternary copper(II) complexes such as (2,2'-bipyridine)(catecholato)copper(II) (abbreviated as [Cu(cat)(bpy)]), and (catecholato)(1,10-phenanthroline)copper(II) ([Cu-(cat)(phen)]), having strong bidentate π-donor and π-acceptor ligands, show very high stability constants.[11–13] As for the solution phenomena such as equilibrium constants and syntheses of ternary copper(II) complexes, a number of papers have

---

*Author for correspondence.

been published, but there are few investigations on electronic transitions except for d-d transitions at low energy.[1-15] Brown *et al.* measured the electronic absorption spectra of some ternary copper(II) catecholate complexes.[16] According to them, both [Cu(cat)(bpy)] and [Cu(cat)(phen)] show relatively intense absorption bands around 500 nm in the crystalline state, corresponding to 450 nm bands in methanol. From X-ray photoelectron data for these complexes, they have suggested that the 450 nm bands are due to MLCT, *i.e.*, intramolecular CT transitions from copper(II) to cat. On the other hand, Benedix *et al.* have reported that the 450 nm band of [Cu(cat)(bpy)] (or [Cu(cat)(phen)]) can be assigned to an interligand CT (LL'CT) transition from cat to bpy (or phen) on the basis of extended Hückel MO calculations.[17] If this is the case, it may be of interest that the two π-electronic systems of cat and bpy (or phen), existing almost independently, can interact with each other. If the bands mentioned above are due to LL'CT transitions, the transition energies of the two complexes must be considerably different. However, in the cases of [Cu(cat)(bpy)] and [Cu(cat)(phen)], the band positions of two bands are almost identical. As described above, several papers on the electronic transitions of [Cu(cat)(bpy)] and [Cu(cat)(phen)] have been published, but the results are not always self-consistent.

In the present investigation, the polarized absorption spectrum of [Cu(cat)(phen)] has been measured with the aid of a stretched polymer film technique to determine polarization directions of the electronic bands.[19-21] Furthermore, the spectrum of [Cu(cat)(phen)] is compared with those of (catecholato)(ethylenediamine)copper(II) ([Cu(cat)(en)]) and (oxalato)(1,10-phenanthroline)copper(II) ([Cu(ox)(phen)]). From these results together with MO calculations, electronic structures and the natures of electronic transitions of [Cu(cat)(phen)] have been clarified.

EXPERIMENTAL

Materials

The ligands catechol, 1,10-phenanthroline, oxalic acid, and ethylenediamine (Wako Pure Chemical Co., Ltd.) were used as supplied. The ternary copper(II) complexes, [Cu(cat)(phen)], [Cu(cat)(en)] and [Cu(ox)(phen)] were synthesized and purified by methods described elsewhere.[6,18] Stretched poly(vinylalcohol) (PVA) films containing sample molecules were prepared by a previously described method.[19-21] Methanol (Wako) was distilled prior to use.

Measurements

Electronic absorption spectra were measured using a Shimadzu UV-3101PC automatic recording spectrophotometer. Polarized absorption spectra were recorded on the above spectrophotometer equipped with a Rochon polarizer. The notations used for the polarization spectra are as follows. $D_{\parallel}$ and $D_{\perp}$ are optical densities measured with light beams polarized parallel to and perpendicular to the stretching direction of the PVA film, respectively; Rd is the ratio of $D_{\parallel}$ and $D_{\perp}$ ($D_{\parallel}/D_{\perp}$); Rs is a stretching ratio of the film.

MO CALCULATIONS

MO calculations were performed by a modified PPP method, which can apply to metal complexes.[22–24] Here, the valence state ionization energies ($I_p(r)$) and electron affinities ($E_a(r)$) for the atoms r are:

$$I_p(C) = 11.22 \text{ eV}, \qquad E_a(C) = 0.62 \text{ eV},$$
$$I_p(N\cdot) = 14.16 \text{ eV}, \qquad E_a(N\cdot) = 1.34 \text{ eV},$$
$$I_p(N:) = 25.00 \text{ eV}, \qquad E_a(N:) = 10.00 \text{ eV},$$
$$I_p(O\cdot) = 17.32 \text{ eV}, \qquad E_a(O\cdot) = 2.65 \text{ eV},$$
$$I_p(O^-) = 25.60 \text{ eV}, \qquad E_a(O^-) = 10.50 \text{ eV}.$$

Two-centre electron repulsion integrals and resonance integrals were evaluated by the Nishimoto-Mataga[25] and Nishimoto-Forster[26] methods respectively. In the MO calculations for the metal complexes, the interactions between two π-electronic systems of the ligands were treated as of through-space, and the resonance integral, β_{NO_-}, between N and O^- is evaluated by the equation,[27]

$$\beta_{NO_-} = 0.42679 S_{NO_-}(I_N + I_{O_-}).$$

Here, S_{NO_-} is an overlap integral between N and O^-, and I_N and I_{O_-} are valence state ionization potentials of N and O^-, respectively. In CI calculations, all the singly excited configurations among the upper eight occupied and lower eight unoccupied orbitals were taken into account. The effects of the d-electron on the π-electronic systems of the ligands have not been taken into account explicity and the central metal ion is treated as a point charge. The magnitude of the point charge is assumed to be $+0.4e$, which is estimated semi-empirically so as to reproduce observed transition energies of the metal complex.[24] Considering that the central copper ion is formally doubly charged ($+2.0e$), the value of $+0.4e$ seems to be rather small. However, the positive charge of the central metal ion is seen to be neutralized greatly by the adjacent two oxide ions of the ligand. Bond lengths and angles were taken from complexes having similar molecular structures.[28–32]

RESULTS AND DISCUSSION

Electronic transitions of [Cu(cat)(en)]

The absorption spectrum of [Cu(cat)(en)] in a 1:1 methanol and water (50% MeOH) and the polarized absorption spectrum in the stretched PVA film are shown in Figure 1. In 50% MeOH, [Cu(cat)(en)] shows absorption bands at 285, 235, and 207 nm (Figure 1a). Moreover, in the region 300–900 nm, weak, broad bands are observed around 400 and 600 nm (the insert in Figure 1a). The 600 nm band is assigned to a d-d transition, as already published.[33,34] The 400 nm band is considered to be due to an LM or MLCT transition, from the results of MO calculations described later. The 285, 235 and 207 nm bands observed in 50% MeOH are red-shifted in the stretched PVA film and observed at 294, 243 and 212 nm, respectively; an additional band appears at 207 nm as a shoulder (Figure 1b). The 294 nm band assumes relatively high Rd values, and the 243 nm band low Rd values. This indicates that the 294 and 243 nm bands are polarized along long and short molecular axes, respectively. Rd values decrease toward the shorter
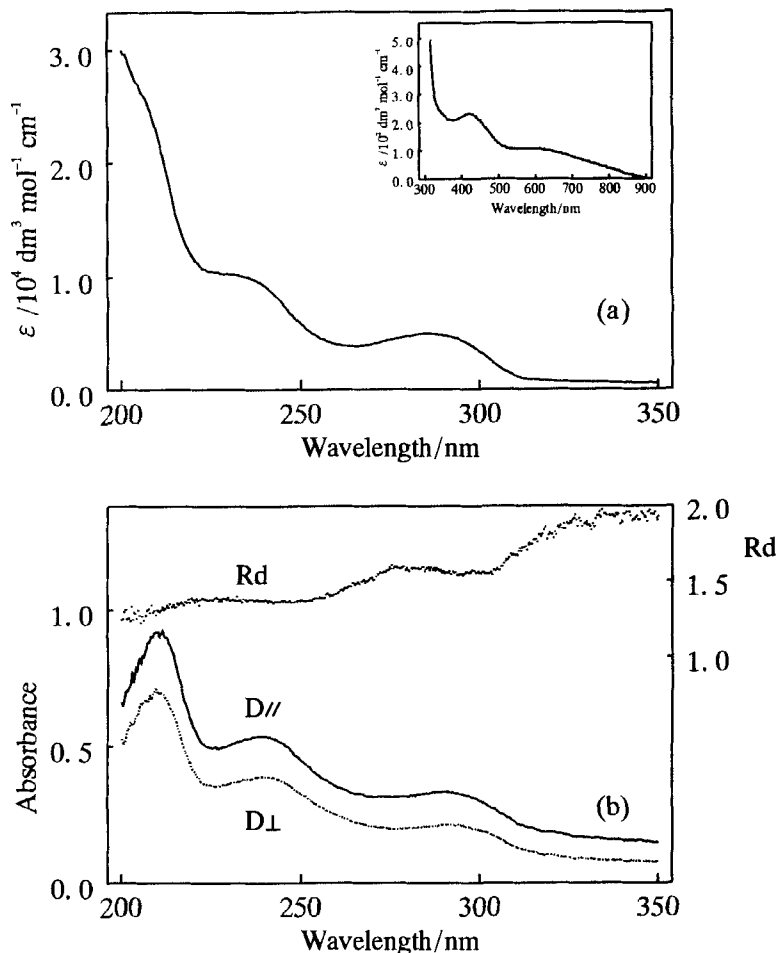
Figure 1 The electronic absorption and polarized absorption spectra of [Cu(cat)(en)]; (a) absorption spectrum of [Cu(cat)(en)] in 50% MeOH; (b) polarized absorption spectrum of [Cu(cat)(en)] in stretched PVA film; Rs = 8.5.

wavelength side in the 212 nm band region. This means that the 212 nm band is an overlap of two transitions polarized along the long and short molecular axes, *i.e.*, the absorption maximum at 212 nm and the shoulder around 207 nm may be due to the long and short axis polarized transitions, respectively. At longer wavelengths than 300 nm, Rd values increase greatly. This means that the adjacent broad band around 400 nm (in 50% MeOH) is polarized along the long molecular axis. These results are compared with MO calculations in Table 1. The long axis polarized 294 and 212 nm bands are assigned to the $\pi\pi^*_1$ and $\pi\pi^*_3$ transitions, respectively, and the short axis polarized 243 and 207 nm ones to the $\pi\pi^*_2$ and $\pi\pi^*_4$ transitions, respectively. The excited state wavefunctions of [Cu(cat)(en)] are given below and

Table 1 Calculated and observed results for the $\pi\pi^*$ transitions of [Cu(cat)(en)].

	Symmetry	Transition energy(nm)		Intensity		Polarization direction	
		calc.	obs.[a]	calc.[b]	obs.[c]	calc.	obs.
$\pi\pi^*_1$	$(^1A_1)$	303.1	294	0.02069	0.296	Z	Z
$\pi\pi^*_2$	$(^1B_1)$	250.2	243	0.14037	0.526	Y	Y
$\pi\pi^*_3$	$(^1A_1)$	212.0	212	1.10101	1.000	Z	Z
$\pi\pi^*_4$	$(^1B_1)$	208.2	207	0.73846	0.884	Y	Y

[a]Observed in PVA film.
[b]Oscillator strength (f).
[c]Relative intensity measured in PVA film.
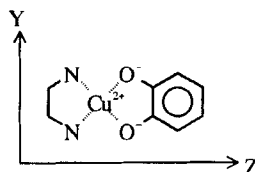
$$\Psi_1 = 0.5958\chi_{6,9} + 0.7980\chi_{7,8} + \cdots$$

$$\Psi_2 = -0.4108\chi_{6,8} + 0.9048\chi_{7,9} + \cdots$$

$$\Psi_3 = 0.7775\chi_{6,9} - 0.5940\chi_{7,8} + \cdots$$

$$\Psi_4 = -0.9064\chi_{6,8} - 0.3961\chi_{7,9} + \cdots$$

MO's of [Cu(cat)(en)] concerned with the above total wavefunctions shown diagrammatically in Figure 2. The main contributors to Ψ_1 and Ψ_3 are $\chi_{6,9}$ and $\chi_{7,8}$, and those to Ψ_2 and Ψ_4 are $\chi_{6,8}$ and $\chi_{7,9}$. Here, $\chi_{i,j}$ is a configurational wavefunction corresponding to one electron excitation from the i'th occupied MO (φ_i) to the j'th vacant one (φ_j).

occupied orbitals

ϕ_6 (a₂) ϕ_7 (b₂)

vacant orbitals

ϕ_8 (b₂) ϕ_9 (a₂)
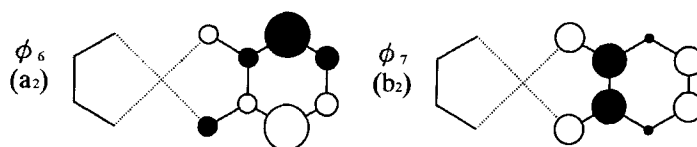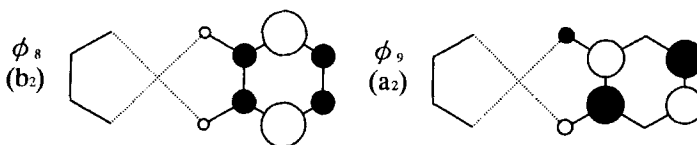
Figure 2 Diagrammatic representations of SCF MO's of [Cu(cat)(en)].

Electronic transitions of [Cu(ox)(phen)]

In 50% MeOH, [Cu(ox)(phen)] shows absorption maxima or shoulders at 345, 329, 314, 294, 272.5, 266, 233, 220, 203.5 and around 650 nm, the latter being assigned to a d-d transition (Figure 3a). In stretched PVA film, the bands corresponding to the 345, 329, 314, 294, 272.5, 266, 233, 220, and 203.5 nm bands in 50% MeOH are observed at 347, 331, 316, 297, 276.0, 268, 234, 225 and 208 nm, respectively (Figure 3b). In the film, guest molecules are usually preferentially oriented in such a manner that the long molecular axes incline towards the stretching direction. However, comparison of experimental and calculated results shows that the short molecular axes of the guest molecules incline preferentially to the stretching direction of the polymer film, *i.e.*, in this case 1,10-phenanthroline moieties in
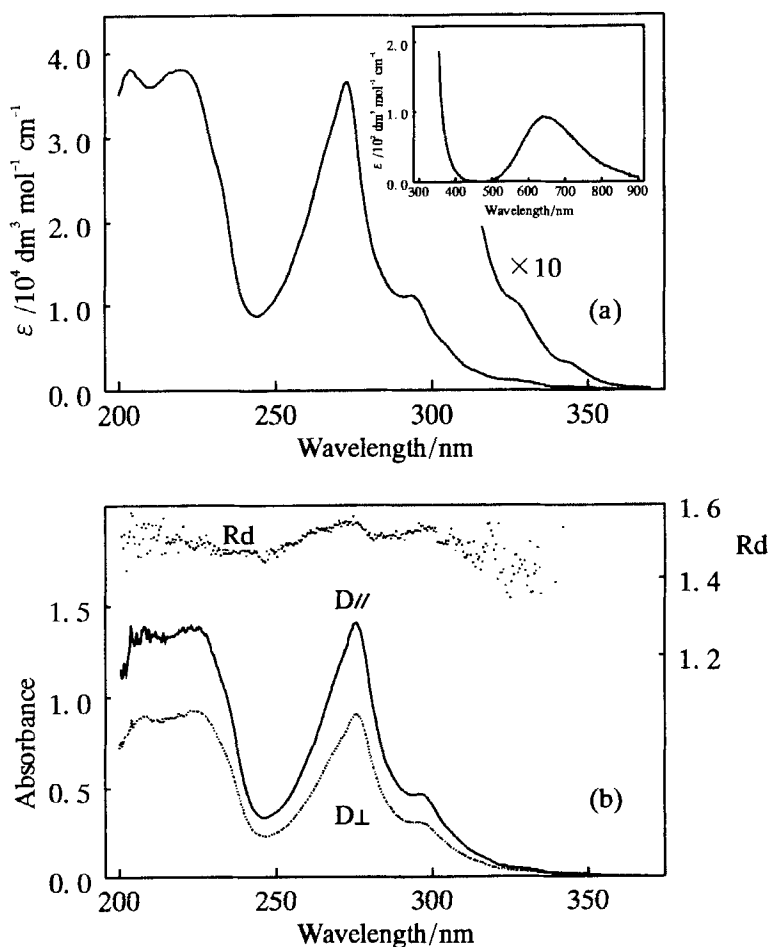
Figure 3 The electronic absorption and polarized absorption spectra of [Cu(ox)(phen)]; (a) absorption spectrum of [Cu(ox)(phen)] in 50% MeOH; (b) polarized absorption spectrum of [Cu(ox)(phen)] in stretched PVA film; Rs = 9.0.

Table 2 Calculated and observed results for the $\pi\pi^*$ transitions of [Cu(ox)(phen)].

	Symmetry	Transition energy(nm)		Intensity		Polarization direction	
		calc.	obs.[a]	calc.[b]	obs.[c]	calc.	obs.
$\pi\pi^*_1$	($^1A_1$)	341.8	347	0.00015	0.032	Z	Z
$\pi\pi^*_2$	($^1B_1$)	312.5	297	0.07745	0.336	Y	Y
$\pi\pi^*_3$	($^1B_1$)	283.8	276.0	0.88316	1.016	Y	Y
$\pi\pi^*_4$	($^1A_1$)	268.6	268	0.29602	0.765	Z	Z
$\pi\pi^*_5$	($^1B_1$)	238.1	225	1.00079	1.000	Y	Y
$\pi\pi^*_6$	($^1A_1$)	238.1	234	0.44277	0.732	Z	Z
$\pi\pi^*_7$	($^1A_1$)	229.5		0.03034		Z	
$\pi\pi^*_8$	($^1B_1$)	218.9		0.01199		Y	
$\pi\pi^*_9$	($^1A_1$)	218.2		0.00026		Z	
$\pi\pi^*_{10}$	($^1B_1$)	210.2		0.00328		Y	
$\pi\pi^*_{11}$	($^1B_1$)	208.9 ⎱ 208		0.13526	1.007	Y	Y + Z
$\pi\pi^*_{12}$	($^1A_1$)	207.5 ⎰		0.52923		Z	

[a]Observed in PVA film.
[b]Oscillator strength (f).
[c]Relative intensity measured in PVA film.
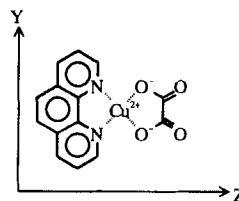
[Cu(ox)(phen)] play an important role in the adsorption of the guest molecules. This indicates that electronic bands with low Rd values are polarized along the long molecular axis (C_2 or Z axis), and the bands with high Rd values along the short molecular axis (perpendicular to C_2 or Y axis). Intervals between the 347 and 331 nm and the 331 and 316 nm bands are almost the same and the latter are considered to be vibronic bands originating at 347 nm. This assignment is supported by the fact that 1,10-phenanthroline shows vibronic bands at 338, 324.0 and 310.0 nm.[35] Since the 316 nm band assumes relatively low Rd values, and the 297 and 276.0 nm bands high values, it is clear that the 316 nm band is polarized along the Z axis, and the 297 and 276.0 nm bands along the Y axis. The Rd values for the 268 nm shoulder band are lower compared with those for the main band at 276.0 nm, indicating that the 268 nm band is polarized along the Z axis. Similarly, it is seen that the 234 and 225 nm bands are polarized along the Z and Y axes, respectively. As for the 208 nm band, the Rd values fluctuate in this region, and the polarization direction cannot be determined. The 347, 297, 276.0, 268, 234 and 225 nm bands are assigned to the $\pi\pi^*_1$, $\pi\pi^*_2$, $\pi\pi^*_3$, $\pi\pi^*_4$, $\pi\pi^*_6$, and $\pi\pi^*_5$, transitions, respectively (Table 2). The observed band at 208 nm may be ascribed as an overlap of the $\pi\pi^*_{11}$ and $\pi\pi^*_{12}$ transitions. In the case of this complex, an LMCT transition between the ligand and metal is likely to arise, but the corresponding CT band cannot be observed. The CT band is probably masked by the strong adjacent $\pi\pi^*$ transitions. The total excited state wavefunctions of [Cu(ox)-(phen)] are as follows.

Y. YAMADA *et al.*

$$\Psi_1 = 0.5890\,\chi_{10,12} - 0.7430\,\chi_{11,13} + \cdots$$

$$\Psi_2 = 0.8114\chi_{11,12} + \cdots$$

$$\Psi_3 = 0.6294\chi_{10,13} - 0.5231\chi_{11,12} + \cdots$$

$$\Psi_4 = 0.6011\chi_{10,12} + 0.6294\chi_{11,13} + \cdots$$

$$\Psi_5 = -0.5264\chi_{10,13} - 0.4383\chi_{10,15} + \cdots$$

$$\Psi_6 = -0.7640\chi_{11,15} - 0.3606\chi_{10,12} + \cdots$$

$$\Psi_7 = 0.6682\chi_{7,12} + 0.4960\chi_{8,13} + \cdots$$

$$\Psi_8 = 0.4724\chi_{10,15} - 0.7688\chi_{11,16} + \cdots$$
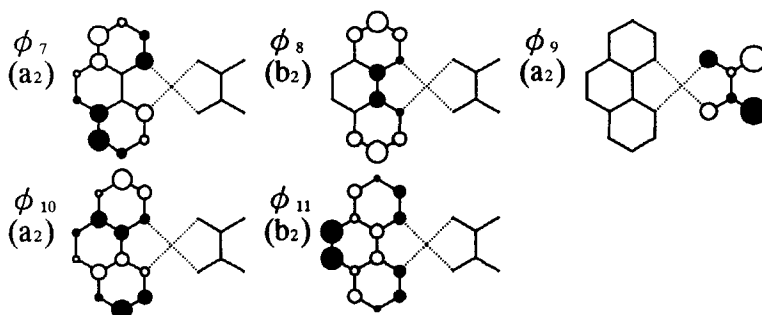
$$\Psi_9 = 0.9937\chi_{11,14} + \cdots$$

$$\Psi_{10} = -0.5878\chi_{8,12} + 0.5032\chi_{9,14} + \cdots$$

$$\Psi_{11} = 0.8571\chi_{9,14} + \cdots$$

$$\Psi_{12} = 0.6372\chi_{8,13} - 0.5567\chi_{10,16} + \cdots$$

The main contributors to Ψ_1 are $\chi_{10,12}$ and $\chi_{11,13}$. Since φ_{10}, φ_{11}, φ_{12} and φ_{13} are localized molecular orbitals on the 1,10-phenanthroline (phen) moiety, the $\pi\,\pi^*{}_1$ transition can be regarded as electronic transition on the phen skeleton (Figure 4).
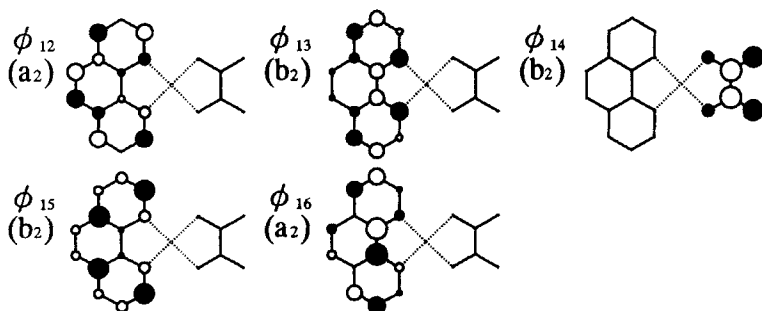
occupied orbitals

vacant orbitals

**Figure 4**   Diagrammatic representations of SCF MO's of [Cu(ox)(phen)].

Similarly, the $\pi\pi^*_2$, $\pi\pi^*_3$, $\pi\pi^*_4$, $\pi\pi^*_5$, $\pi\pi^*_6$, and $\pi\pi^*_{12}$ transitions are due to localized transitions on the phen skeleton. On the other hand, the main contributor to Ψ_{11} corresponding to the $\pi\pi^*_{11}$ transition is $\chi_{9,14}$. Therefore, the $\pi\pi^*_{11}$ transition can be regarded as a localized electronic transition on the ox moiety. Though the $\pi\pi^*_9$ transition is LL'CT from phen (φ_{11}) to ox (φ_{14}), the corresponding band could not be observed.
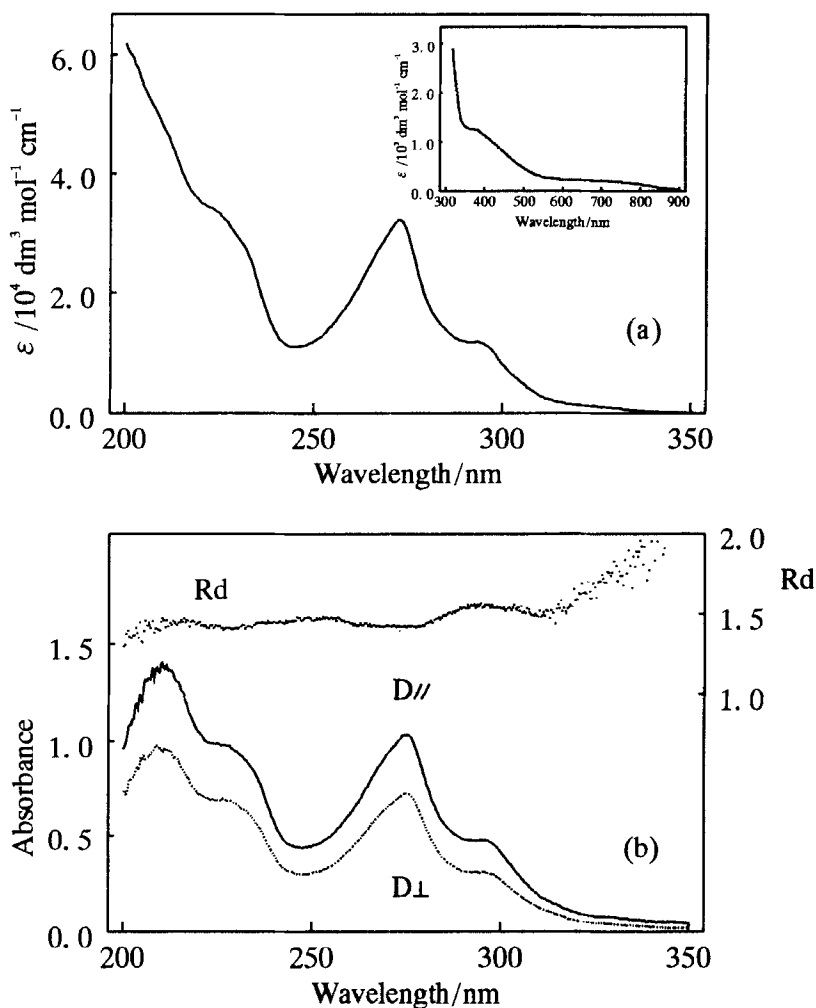
Figure 5 The electronic absorption and polarized absorption spectra of [Cu(cat)(phen)]; (a) absorption spectrum of [Cu(cat)(phen)] in 50% MeOH; (b) The polarized absorption spectrum of [Cu(cat)(phen)] in stretched PVA film; Rs = 8.8.

**Table 3** The calculated and observed results for the $\pi\pi^*$ transitions of [Cu(cat)(phen)].

	Symmetry	Transition energy(nm)		Intensity		Polarization direction	
		calc.	obs.[a]	calc.[b]	obs.[c]	calc.	obs.
$\pi\pi^*_1$	$(^1A_1)$	338.9	331	0.00009	0.054	Z	Z
$\pi\pi^*_2$	$(^1B_1)$	310.9	308	0.09006	0.340	Y	Y
$\pi\pi^*_3$	$(^1A_1)$	304.1	295	0.03230	0.339	Z	Z
$\pi\pi^*_4$	$(^1A_1)$	302.8		0.00027		Z	
$\pi\pi^*_5$	$(^1B_1)$	300.4		0.00004		Y	
$\pi\pi^*_6$	$(^1B_1)$	283.7	275.0	0.72271	0.737	Y	Y
$\pi\pi^*_7$	$(^1A_1)$	266.8	267	0.33588	0.607	Z	Z
$\pi\pi^*_8$	$(^1B_1)$	251.1		0.10890		Y	
$\pi\pi^*_9$	$(^1A_1)$	246.3		0.00015		Z	
$\pi\pi^*_{10}$	$(^1B_1)$	245.4		0.00129		Y	
$\pi\pi^*_{11}$	$(^1A_1)$	237.7	233	0.51053	0.631	Z	Z
$\pi\pi^*_{12}$	$(^1B_1)$	237.3	227	1.01670	0.696	Y	Y
$\pi\pi^*_{13}$	$(^1A_1)$	231.9		0.00006		Z	
$\pi\pi^*_{14}$	$(^1A_1)$	228.3		0.03819		Z	
$\pi\pi^*_{15}$	$(^1B_1)$	218.3		0.00104		Y	
$\pi\pi^*_{16}$	$(^1A_1)$	212.4	210.0	1.28175	1.000	Z	Z
$\pi\pi^*_{17}$	$(^1B_1)$	209.3	209	0.74444	0.979	Y	Y

[a]Observed in PVA film.
[b]Oscillator strength.
[c]Relative intensity measured in PVA film.
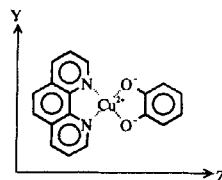
Electronic transitions of [Cu(cat)(phen)]

This complex shows two absorption bands around 650 and 400 nm in the wavelength region 300–900 nm in 50% MeOH (the inserted picture in Figure 5a). It is obvious that the 650 nm band is due to a d-d transition. Absorption corresponding to the 400 nm band of [Cu(cat)(phen)] also appears in the spectrum of [Cu(cat)(en)], but is not seen in the spectrum of [Cu(ox)(phen)]. This may indicate that the 400 nm band of [Cu(cat)(phen)] is due to an intramolecular CT transition between copper(II) and cat. In the region 200–350 nm, [Cu(cat)(phen)] shows absorption bands at 329, 314, 305, 294, 272.5, 233 and 224 nm (Figure 5a). The spectrum of [Cu(cat)(phen)] in this region is similar to the sum of the spectra of [Cu(cat)(en)] and [Cu(ox)(phen)]. As described in the previous section, [Cu-(cat)(en)] and [Cu(ox)(phen)] do not show intramolecular CT bands. Thus, the absorption bands of [Cu(cat)(phen)] in this wavelength region can be attributable to localized electronic transitions on the ligands. In stretched PVA film, the bands corresponding to the 329, 314, 305, 294, 272.5, 266, 233 and 225 nm bands observed in 50% MeOH appear at 331, 316, 308, 295, 275.0, 267, 233 and 227 nm, respectively (Figure 5b). Furthermore, an intense band is observed at 210.0 nm. According to MO calculations, the C_2 axis of the [Cu(cat)(phen)] molecule, contrary to the case with [Cu(ox)(phen)], orients preferentially to the stretching direction of the PVA film. The Rd curve shows a minimum around 308 nm, and a maximum
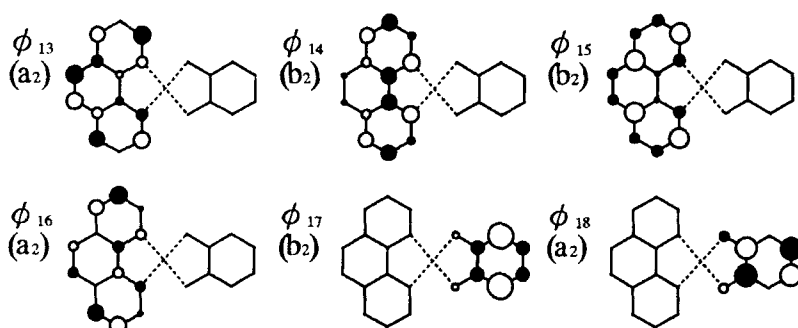
occupied orbitals
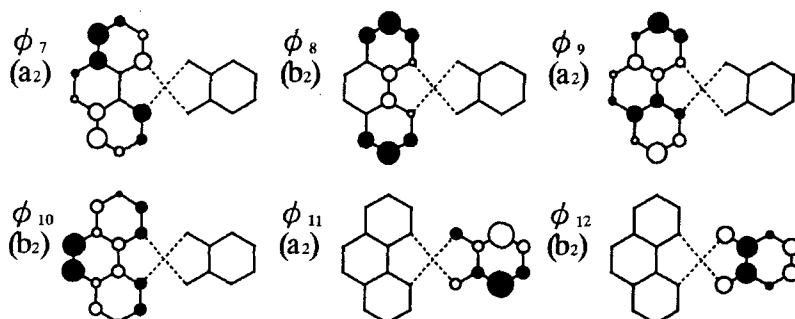
vacant orbitals

Figure 6 Diagrammatic representations of SCF MO's of [Cu(cat)(phen)].

around 295 nm, indicating that the corresponding bands are polarized along short (Y) and long molecular (Z) axes, respectively. Since the Rd values for the 275.0 nm band are low, the 275.0 nm band is polarized along the Y axis. The shoulder at 267 nm is considered to be due to a different electronic transition from the main band at 275.0 nm by analogy with [Cu(ox)(phen)]. The 233 and 227 nm bands are polarized along the Z and Y axes, respectively, because the Rd values for the 233 nm band are higher than those for the 227 nm band. The Rd values decrease toward the short wavelength side of the most intense 210.0 nm band; band maxima of the $D_{\parallel}$ and $D_{\perp}$ curves are at 210.0 and 209 nm, respectively. These experimental results show that the 210.0 and 209 nm bands may be due to different electronic transitions, i.e., the 210.0 nm band is polarized along the Y axis, and the 209 nm band along the Z axis. The 331, 308, 295, 275.0, 267, 233, 227, 210.0 and 209 nm bands may correspond to the calculated $\pi \pi^*_1$, $\pi \pi^*_2$, $\pi \pi^*_3$, $\pi \pi^*_6$ $\pi \pi^*_7$, $\pi \pi^*_{11}$, $\pi \pi^*_{12}$, $\pi \pi^*_{16}$, and $\pi \pi^*_{17}$ transitions, respectively (Table 3). The excited state wavefunctions of [Cu(cat)(phen)] are given below.

$$\Psi_1 = -0.5960\ \chi_{9,13} + 0.7419\ \chi_{10,14} + \cdots$$

$$\Psi_2 = 0.5324\ \chi_{9,14} + 0.8228\ \chi_{10,13} + \cdots$$

$$\Psi_3 = -0.5731\ \chi_{11,18} + 0.7941\ \chi_{12,17} + \cdots$$

$$\Psi_4 = 0.9666\ \chi_{12,14} + \cdots$$

$$\Psi_5 = 0.9876\ \chi_{12,13} + \cdots$$

$$\Psi_6 = -0.6307\ \chi_{9,14} + 0.4999\ \chi_{10,13} \cdots$$

$$\Psi_7 = 0.6021\ \chi_{9,13} + 0.6307\ \chi_{10,14} + \cdots$$

$$\Psi_8 = 0.3953\ \chi_{11,17} + 0.8893\ \chi_{12,18} + \cdots$$

$$\Psi_9 = 0.9696\ \chi_{11,13} + \cdots$$

$$\Psi_{10} = -0.9912\ \chi_{11,14} + \cdots$$

$$\Psi_{11} = -0.3495\ \chi_{9,13} + 0.7708\ \chi_{10,15} + \cdots$$

$$\Psi_{12} = 0.3609\ \chi_{7,14} - 0.5387\ \chi_{9,14}$$
$$+ 0.4326\ \chi_{9,15} + 0.3890\ \chi_{10,15} + \cdots$$

$$\Psi_{13} = 0.9610\ \chi_{12,15} + \cdots$$

$$\Psi_{14} = 0.6817\ \chi_{7,13} - 0.4684\ \chi_{8,14}$$
$$+ 0.3471\ \chi_{9,16} + \cdots$$

$$\Psi15 = 0.4649\ \chi_{9,15} - 0.7696\ \chi_{10,16} + \cdots$$

$$\Psi_{16} = -0.7469\ \chi_{11,18} + 0.5564\ \chi_{12,17} + \cdots$$

$$\Psi_{17} = -0.4204\ \chi_{7,14} + 0.5337\ \chi_{8,13}$$
$$+ 0.6179\ \chi_{11,17} \cdots$$

The main contributors to the state wavefunction Ψ_1, which corresponds to $\pi\pi^*_1$, are $\chi_{9,13}$ and $\chi_{10,14}$. Molecular orbitals φ_9, φ_{10}, φ_{13}, and φ_{14} are localized on the phen moiety, so that the $\pi\pi^*_1$ transition is regarded as a localized electronic transition on phen (Figure 6). Similarly, the $\pi\pi^*_2$, $\pi\pi^*_6$, $\pi\pi^*_7$, $\pi\pi^*_{11}$ and $\pi\pi^*_{12}$ transitions are considered to be localized on phen. On the other hand, the main contributors to Ψ_3 and Ψ_{16} are $\chi_{11,18}$ and $\chi_{12,17}$, and φ_{11}, φ_{12}, φ_{17}, and φ_{18} are localized on the cat moiety. Therefore, the $\pi\pi^*_3$ and $\pi\pi^*_{16}$ transitions are localized on cat. The main contributors to Ψ_{17}, corresponding to the observed 209 nm band, are $\chi_{7,14}$ $\chi_{8,13}$ and $\chi_{11,17}$, of which $\chi_{7,14}$ and $\chi_{8,13}$ correspond to one electron excitations in phen and $\chi_{11,17}$ to excitation in cat. This indicates that the excited state represented by Ψ_{17} is a superimposition of the two local excitations on phen and cat. Thus the two independent π-electronic systems interact greatly with each other through configuration interactions. Calculated electronic transitions $\pi\pi^*_4$ and $\pi\pi^*_5$ are LL'CT transitions from cat to phen, but the corresponding bands are not observed.

Acknowledgements

References

1. R. Griesser and H. Sigel, *Inorg. Chem.*, **9**, 1238 (1970).
2. P.R. Huber, R. Griesser and H. Sigel, *Inorg. Chem.* 10, 945 (1971).
3. H. Sigel, P.R. Huber and R.F. Pasternack, *Inorg. Chem.*, **10**, 2226 (1971).
4. R. Griesser and H. Sigel, *Inorg. Chem.*, **10**, 2229 (1971).
5. P.R. Huber and H. Sigel, *Z. Naturforsch. B*, **27**, 1319 (1972).
6. F.A. Walker, H. Sigel and D.B. McCormick, *Inorg. Chem.*, **11**, 2756 (1972).
7. H. Sigel, P.R. Huber, R. Griesser and B. Prijs, *Inorg. Chem.*, **12**, 1198 (1973).
8. H. Sigel, R. Caraco and B. Prijs, *Inorg. Chem.*, **13**, 462 (1974).
9. C.F. Naumann and H. Sigel, *J. Am. Chem. Soc.*, **96**, 2750 (1974).
10. H. Sigel and B. Prijs, *Chimia*, **29**, 134 (1975).
11. H. Sigel, *Angew. Chem. Int. Ed. Engl.*, **14**, 394 (1975).
12. I.P. Mavani, C.R. Jejurkar and P.K. Bhattacharya, *J. Indian Chem. Soc.*, **49**, 469 (1972).
13. I.M. Procter, B.J. Hathaway and P.G. Hodgson, *J. Inorg. Nucl. Chem.*, **34**, 3689 (1972).
14. M.S. Mohan, D. Bancroft and E.H. Abbott, *Inorg. Chem.*, **18**, 344 (1979).
15. V. Srivastava and H.L. Nigam, *J. Indian Chem. Soc.*, **59**, 251 (1982).
16. D.G. Brown, W.J. Hughes and G. Knerr, *Inorg. Chim. Acta*, **46**, 123 (1980).
17. R. Benedix and A. Vogler, *Inorg. Chim. Acta*, **204**, 189 (1993).
18. D.G. Brown, J.T. Reinprecht and G.C. Vogel, *Inorg. Nucl. Chem. Lett.*, **12**, 399 (1976).
19. T. Hoshi and Y. Tanizaki, *Z. Phys. Chem., Neue Folge*, **71**, 230 (1970).
20. T. Hoshi, J. Okubo, T. Kawashima, K. Iijima, H. Inoue and T. Sakurai, *Nippon Kagaku Kaishi*, 1 (1987).
21. T. Hoshi, T. Kawashima, J. Okubo, M. Yamamoto and H. Inoue, *J. Chem. Soc., Perkin Trans. II*, 1147 (1986).
22. R. Pariser and R.G. Parr, *J. Chem. Phys.*, **21**, 466, 767 (1953).
23. J.A. Pople, *Proc. Phys. Soc. (London) A*, **68**, 81 (1955).
24. T. Hoshi, Y. Inomaki, M. Wada, Y. Tamada, J. Okubo, M. Kobayashi and H. Inoue, *Ber. Bunsenges. Phys. Chem.*, **98**, 585 (1994).
25. N. Mataga and K. Nishimoto, *Z. Phys. Chem., Neue Folge*, **13**, 140 (1957).
26. K. Nishimoto and L.S. Forster, *Theor. Chem. Acta*, **3**, 407 (1965).
27. N. Bodor, M.J.S. Dewar, A. Harget and E. Haselbach, *J. Am. Chem. Soc.*, **92**, 3854 (1970).
28. C.G. Pierpoint and R.M. Buchanan, *Coord. Chem. Rev.*, **38**, 45 (1981).
29. W. Fitzgerald, J. Fooley, D. McSweeney, N. Ray, D. Sheanon, S. Tyagi, B. Hathaway and P. O'Brien, *J. Chem. Soc., Dalton Trans.*, 1117 (1982).
30. M. Julve, J. Faus, M. Verdauguer and A. Gleizes, *J. Am. Chem. Soc.*, **106**, 8306 (1984).
31. A. Fabretti, G. Franchini. P. Zannini and M. Divaira, *Inorg. Chim. Acta*, **105**, 187 (1985).
32. I. Castro, J. Faus, M. Julve, M.C. Munoz, W. Diaz and X. Solans, *Inorg. Chim. Acta*, **179**, 59 (1991).
33. B.N. Figgis, *"Introduction to Ligand Fields"*, (John Wiley, New York, 1966).
34. K. Sone, S. Utsuno and T. Ogura, *J. Inorg. Nucl. Chem.*, **31**, 117 (1969).
35. T. Hoshi, H. Inoue, J. Yoshino, T. Masamoto and Y. Tanizaki, *Z. Phys. Chem., Neue Folge*, **81**, 23 (1972).